Statistics of Multiple Particle Breakage Accounting for Particle Shape

Priscilla J. Hill
Dave C. Swalm School of Chemical Engineering, Mississippi State University, Mississippi State, MS 39762

DOI 10.1002/aic.10091
Published online in Wiley InterScience (www.interscience.wiley.com).

A method is presented for developing multiple particle breakage distribution functions that include the shape factor, as well as the particle size. The technique is to first develop a joint probability distribution that accounts for the size and shape factor of each child particle. This is then reduced by successive integration to the marginal probability used in the breakage equation. This technique guarantees mass conservation and exchangeability of child particles while allowing the user to choose the number of child particles formed per breakage. It also allows the user to choose the functional form for the size distribution of particles as well as independently choosing the functional form for the shape factor distribution of particles. To solve the breakage equation, a discretization method is used that conserves particle mass during breakage and correctly predicts changes in the total number of particles. Simulation results show that the shape distribution functions may yield distinguishable shape factor profiles after crushing. Comparison with experimental data indicates that these theoretical functions can be used to model real systems. © 2004 American Institute of Chemical Engineers *AIChE J,* 50: 937–952, 2004
Keywords: population balance equations, breakage, solids processing, particle size distribution, shape factor distribution

Introduction

Particle breakage is of interest because it occurs both naturally and in many manufacturing processes. These processes span a range of industries including pharmaceuticals, pigments, agricultural chemicals, and foods. It is of particular interest in chemical processing plants because it can have a strong impact on unit operations. Breakage may be beneficial and intentional as in the case of crushing; or it may be detrimental and unintentional as in the case of fragmentation and attrition in fluidized bed reactors and combustors (Shamlou et al., 1990).

It is imperative that key morphological properties be included in modeling breakage. Although there are a variety of morphological properties that can be studied, particle size and shape are of primary importance because they determine a wide range of physical and chemical properties. Both the particle size distribution (PSD) and the particle shape have a strong effect on particle product quality. For example, the bioavailability of pharmaceuticals often depends on both the particle size and shape. In heterogeneous catalysis, shape is important because it affects catalyst effectiveness (Buffham, 2000). For paint, opacity is a function of size, whereas coating layer properties are a function of the shape distribution (Lohmander, 2000b); for example, a broader shape factor distribution produces a coating with higher mechanical strength. Process operability can also be a strong function of both particle size and shape. It is known that filtration rates are a function of PSD, and that flat plates will have low filtration rates compared to those of spheres. In addition, particle shape strongly affects the flowability of particulates (Mersmann, 2001; Scanlon and Lamb, 1995). Because both particle size and shape can strongly affect product quality and process operability, it is necessary to account for their effects in modeling and design.

Particle shape is often neglected in modeling breakage, although it can have a significant effect on unit operation. For example, attrition has a significant effect in crystallizer operation not only because it produces small particles (Gahn and

P. J. Hill's e-mail address is phill@che.msstate.edu.

Table 1. Shape Factors and Shape Coefficients

Name	Symbol	Definition	Source
Volume shape factor	ϕ_v	$v = \phi_v L^3$	Allen (1975), Mullin (2001), Mersmann (2001)
Surface shape factor	ϕ_s	$s = \phi_s L^2$	Allen (1975), Mullin (2001), Mersmann (2001)
Sphericity		$\frac{(6\phi_v/\pi)^{2/3}}{\phi_s/\pi}$	Mullin (2001), Mersmann (2001)
Sphericity	ϕ_0	$\phi_0^2 = d/D$	Scanlon and Lamb (1995)
Sphericity	ψ	$\frac{(6v/\pi)^{2/3}}{(s/\pi)^{1/2}}$	Allen (1975)
Roundness		$\frac{(\text{perimeter})^2}{4\pi(\text{area})}$	Mazzarotta, Di Cave, and Bonifazi (1996)
Elongation ratio		$\frac{\text{width}}{\text{length}}$	Allen (1975)
Flakiness ratio		$\frac{\text{length}}{\text{height}}$	Allen (1975)
Overall shape factor	F	$F = \frac{\phi_s}{\phi_v}$	Mersmann (2001)
Resistance shape factor	K_R	$R_f = 3\pi\mu L K_R u$	Kousaka, Okuyama, and Payatakes (1981)
Dynamic shape factor	κ	$\frac{(6v/\pi)^{2/3}(\rho_p - \rho_f)g}{18\mu u_t}$	Kousaka, Okuyama, and Payatakes (1981)

Mersmann, 1999; Gahn et al., 1996; Mazzarotta et al., 1996; Shamlou et al., 1990), but also because it influences the size and shape of all of the crystals. Mersmann (2001) further states that, although attrition will produce more rounded particles, it will also produce many fines that will reduce the flowability. Much of the earlier literature that covers breakage in stirred vessels studies the effect of breakage on the PSD (Conti and Nienow, 1980; Mazzarotta, 1992; Nienow and Conti, 1978; Synowiec et al., 1993), but does not include particle shape. Later research by Mazzarotta et al. (1996) investigates the effects of time on sugar crystal attrition and determined that the larger crystals became more rounded with time. More recent research by Bravi et al. (1999) focuses more on the particle shape. They conclude that the remaining large particles had an aspect ratio close to unity, whereas the fine particles became more needle shaped. Although this research used the parameters of roundness and aspect ratio, these parameters were not incorporated into modeling.

To better design processes, it is necessary to model the changes in particle shape as well as the changes in particle size. As discussed by Wintermantel (1999), following changes in composition is not sufficient; it is critical to follow the changes in particle attributes through the entire process. This requires quantitative information on particle breakage. As described above, most of the work on particle shape has been qualitative rather than quantitative. To quantitatively incorporate particle shape into modeling, it is necessary to have simulation and design tools based on population balance equations (PBEs). Although PBEs are often used to follow one particle property (usually size), additional properties must be included in the PBEs to accurately follow particle attributes. For breakage, the shape factor must be directly incorporated in the multiple particle breakage distribution functions used in PBEs. Current simulation and design tools do not have these capabilities. Therefore, research is needed to correct these omissions and make the simulations more physically realistic.

The main goal of this research is to address this deficiency by providing a mathematical basis for incorporating particle size and shape into modeling breakage. This is accomplished by providing a procedure for correctly incorporating particle shape into the breakage distribution function used in the breakage PBE. To ensure exchangeability of child particles, the first step is to use a joint probability that considers the sizes and the shape factors of all of the particles. This may be reduced by integration to a marginal probability that can be used in the breakage equation. The development of breakage distribution functions is first demonstrated for the case of binary breakage and is then extended to multiple particle breakage. Various functional forms for the distribution function are generated and compared. Simulations are then performed to show the variation in resulting shape distributions after grinding. Finally, simulation results using one of the newly developed breakage distribution functions are compared against experimental data.

Literature Review

Shape factor

Ennis et al. (1994) state that morphological considerations, including both particle size and shape, are the primary considerations in particle technology. They further state that because few particles are spherical, there is often the need for specialized dimensions.

One of the most common definitions of the shape factor is

$$\phi_v = v/L^3 \tag{1}$$

where ϕ_v is the shape factor, v is the particle volume, and L is the characteristic particle length. The purpose of ϕ_v in this case is to relate the characteristic length to the particle volume. This shape factor is equal to 1 in the case of a cube and equal to $\pi/6$ when L is the diameter of a sphere.

There are a variety of approaches in the literature for handling the particle shape, depending on the purpose of the shape factor. Selected shape factors are shown in Table 1, where v is the particle volume, L is the representative particle length, and s is the particle surface area. For example, researchers primarily interested in the particle surface area rather than the volume

developed a surface area shape factor ϕ_s based on the particle surface area (Mullin, 2001).

Other shape factors aim to provide information about the shape of the particle. Scanlon and Lamb (1995) used a definition for sphericity to compare shapes. In this case, the sphericity is determined from a 2-D image of the particle according to the following formula

$$\phi_0^2 = d/D \tag{2}$$

where D is the diameter of the smallest circle that circumscribes the particle image and d is the diameter of the largest circle that will fit inside the particle image. For this analysis, the particle is resting so that its maximum cross-sectional area is shown in the image. The purpose of sphericity is to determine how close the particle is to being a sphere. Other definitions for sphericity use ϕ_v and ϕ_s (Mullin, 2001), the volume and surface area shape factors, respectively.

Shape descriptions also include roundness (Mazzarotta et al., 1996) as well as aspect ratios (Allen, 1975), such as the elongation ratio and the flakiness ratio. In these aspect ratios, it is assumed that the particle is resting on the surface of maximum stability. The terms width, height, and length refer to the dimensions of a rectangular parallelepiped that circumscribe the particle.

Other shape factors are concerned with a particle's flow properties in a liquid. The resistance shape factor (Kousaka et al., 1981) is used to determine the Stokes flow resistance, R_f. The dynamic shape factor (Kousaka et al., 1981) is the ratio of the drag force on a particle to the drag force on a sphere of the same volume. In this definition ρ_p and ρ_f are the particle and fluid densities, μ is the fluid viscosity, and u_t is the gravitational settling velocity. If the particle is a sphere, the shape factor is equal to one.

Breakage equation and functions

A familiar form of the breakage equation expresses the change in the number density at a given volume, $n(v)$, as the combination of a birth term and a death term. The birth term accounts for particles being formed in the range of v to $v + dv$ from larger particles breaking, whereas the death term accounts for the removal of particles from this interval by particles breaking into smaller particles. This is expressed mathematically as

$$\frac{\partial n(v)}{\partial t} = \int_v^\infty b'_v(v, w)S(w)n(w)dw - S(v)n(v) \tag{3}$$

where v and w are particle volumes; $n(v)$ is the population density function; $S(v)$ is the specific rate of breakage of particles of volume v; and $b'_v(v, w)$ is the breakage distribution function, which indicates how many particles of volume v are formed when parent particles of volume w are broken. Although the population density is also a function of time, t, this will not be listed explicitly in this article. This breakage equation does not incorporate particle shape.

Previous work was done on the breakage of a single particle into multiple child particles (Hill and Ng, 1996). Their work developed the idea that a multivariate joint probability is needed to represent the breakage distribution function. This joint probability listed the parent particle volume and all of the child particle volumes except for one child particle volume. The reason for this was that the final child particle volume could be calculated from the volumes of the parent particle and the other child particles. They further stated that this breakage function had to meet three constraints: number prediction, mass conservation, and exchangeability. The number prediction constraint allowed one to develop a function so that p child particles were formed when a parent particle was broken. The mass conservation constraint guaranteed that mass was conserved when a particle broke. The exchangeability constraint stated that the value of the breakage distribution function could not change when the child particle information was entered into the distribution function in a different order. By successive integration the multivariate joint probability was reduced to a marginal probability in terms of a single child particle volume in addition to the parent particle volume.

There are two sets of expressions that were developed by Hill and Ng (1996) to meet these constraints. One set is the product function with a power law form. In this case the breakage distribution function was given by

$$b_v(v_1, v_2, \ldots, v_{p-1}, w) = \frac{p[m + (m + 1)(p - 1)]!v_1^m v_2^m \cdots v_{p-1}^m (w - \sum_{i=1}^{p-1} v_i)^m}{(m!)^p w^{pm+p-1}} \tag{4}$$

where m is a nonnegative integer constant and v_i is the volume of the ith child particle. This was reduced to the conventional breakage function of

$$b'_v(v, w) = \frac{pv^m(w - v)^{m+(m+1)(p-2)}[m + (m + 1)(p - 1)]!}{w^{pm+p-1}m![m + (m + 1)(p - 2)]!} \tag{5}$$

A second set is the summation function with a power law form. In this case the breakage distribution function was given by

$$b(v_1, v_2, \ldots, v_{p-1}, w) = \frac{A_{m,p}[\sum_{i=1}^{p-1} v_i^m + (w - \sum_{i=1}^{p-1} v_i)^m]}{w^{m+p-1}} \tag{6}$$

where

$$A_{m,2} = m + 1 \tag{7}$$

and for $p > 2$ there was the following recursive relationship

$$\frac{p}{A_{m,p}} = \frac{(p - 2)!m!}{(m + p - 1)!} \prod_{i=0}^{p-3} \frac{1}{i + 1} + \left(\frac{p - 1}{A_{m,p-1}}\right) \frac{1}{m + p - 1} \tag{8}$$

The summation function was reduced to the conventional breakage function to yield

$$b'_v(v, w) = \frac{m+1}{w^{m+1}}\left[v^m + (w - v)^m\right] \tag{9}$$

for $p = 2$ and

$$b'_v(v, w) = \frac{A_{m,p}}{w^{m+p-1}}\left[v^m(w - v)^{p-2}\prod_{i=0}^{p-3}\frac{1}{i+1} + (w - v)^{m+p-2}\left(\frac{p-1}{A_{m,p-1}}\right)\right] \tag{10}$$

for $p > 2$. Although these are not the only sets of equations to model multiple particle breakage, they do provide enough flexibility to model empirical breakage data.

Diemer and Olson (2002) generalized these product and summation functions using the gamma and beta functions with parameters q_i and r_i. As discussed, not all values of parameters q_i and r_i satisfy the exchangeability constraint.

Multivariate models

Researchers have developed multidimensional PBEs for various applications including crystal growth (Hulburt and Katz, 1964), mass transfer in liquid–liquid dispersions (Ramkrishna, 2000), and microbial populations (Ramkrishna, 2000). Recent work in crystallization by Puel et al. (1997) developed a PBE where the internal coordinates were the length and the width of needle shaped particles. Later work (Gerstlauer et al., 2001) developed a population balance model based on the two internal coordinates of representative crystal length and molar lattice strain of the crystals.

Diemer (1999) developed breakage distribution functions, $b_A(v, A_v; w, A_w)$, that correctly predicted child particle volume v and surface area A_v given the parent particle volume w and surface area A_w. He correctly noted that, although mass will be conserved during breakage, surface area is not necessarily conserved. In his approach he determined the breakage distribution $b_A(v, A_v; w, A_w)$ as the product of the breakage distribution function for size only, $b'_v(v; w)$, and a conditional distribution assuming a given child particle size, $b_a(A_v; v, w, A_w)$. The factor $b'_v(v; w)$ determined the distribution of child particles formed given the parent particle size, whereas the factor $b_a(A_v; v, w, A_w)$ determined the distribution of the child particle surface area given the child particle volume and the parent particle attributes. Breakage distribution functions that include both the particle size and the volumetric shape factor are not available for particle breakage.

The objective of this work is to develop a bivariate approach for particle breakage that takes into account the volumetric shape factor as well as the particle volume. This will allow one to follow both particle size and shape in a chemical manufacturing process. In the following sections a systematic procedure is presented for developing appropriate bivariate breakage distribution functions.

Theoretical Breakage Functions Incorporating Shape

Theoretical breakage functions that account for shape may be developed for different numbers of child particles produced. To illustrate the basic concepts of the resulting shape factor distribution from particle breakage, binary breakage is discussed first. This is followed by an extension to multiparticle breakage.

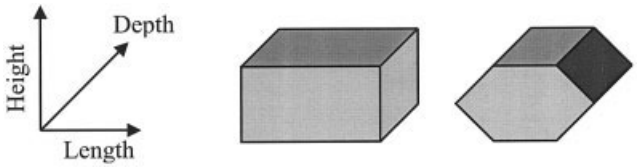

Figure 1. Two crystals with the same length, height, and depth.

Breakage equation

To account for particle shape, a shape factor can be added to the terms in Eq. 3. The number density $n(v)$ becomes the number density function including shape, $n_\phi(v, \phi_v)$, where v is the particle volume of interest and ϕ_v is the shape factor of a particle of volume v. To distinguish between the functions in the conventional breakage equation (Eq. 3), and the functions in the breakage equation that includes the shape factor, the subscript "ϕ" is added to the functions that include the shape factor. The breakage equation is rewritten as

$$\frac{\partial n_\phi(v, \phi_v)}{\partial t} = \int_v^\infty \int_{\phi_{w,\min}}^{\phi_{w,\max}} b'_\phi(v, \phi_v, w, \phi_w) S_\phi(w, \phi_w) \times n_\phi(w, \phi_w) d\phi_w dw - S_\phi(v, \phi_v) n_\phi(v, \phi_v) \tag{11}$$

where $S_\phi(v, \phi_v)$ is the specific breakage rate for particles of volume v and shape factor ϕ_v, and $b_\phi(v, \phi_v, w, \phi_w)$ is the breakage distribution function that determines the number of particles of volume v and shape ϕ_v formed when particles of volume w and shape ϕ_w break.

Shape factor

In recent work, researchers have reported crystal sizes in terms of the length along each axis. Although this provides information about the crystal morphology, it does not allow one to determine the crystal volume unless the crystal is a rectangular parallelepiped. An example of this is shown in Figure 1, where both crystals have the same length, height, and depth, although they do not have the same volume. Chemical engineers are usually interested in conserving mass. Because mass is directly proportional to the volume, it is necessary to know the actual particle volume as well as the overall dimensions. In the following development, the shape factor is defined as

$$\phi_v = \frac{v}{L_x L_y L_z} \tag{12}$$

where L_i is the length of the particle along the i axis. This allows researchers to relate an apparent volume, $L_x L_y L_z$, to the actual volume v. In general, if ϕ_v is unity, the particle is a cuboid. If ϕ_v is significantly less that unity, the particle may be dendritic in morphology.

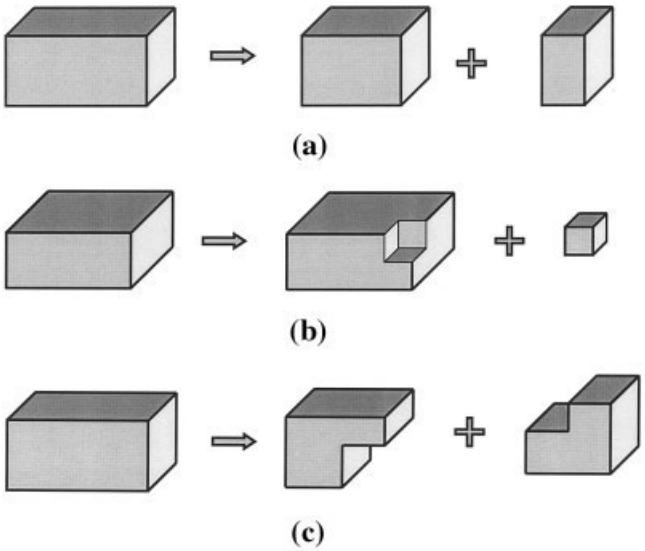

Figure 2. Breakage of parent particle into two child particles: (a) breakage of cuboid into two cuboids; (b) breakage of cuboid into one noncuboid and one cuboid; (c) breakage of cuboid into two noncuboid particles.

Binary breakage

Let us assume that the parent particle has volume w and shape factor ϕ_w. Let us further assume that the two child particles have volumes v_1 and v_2 with shape factors ϕ_1 and ϕ_2, respectively. We know that

$$w = v_1 + v_2 \tag{13}$$

Therefore, if two particle volumes are specified, the other particle volume can be calculated.

However, there is no such relationship between the shape factors. Examples of this are shown in Figure 2, where the parent particle is a rectangular parallelepiped with volume w and a shape factor of $\phi_w = 1$. In Figure 2(a), the two child particles formed are both rectangular parallelepipeds with shape factors equal to 1. In Figure 2(b), one child particle has volume v_1 and a shape factor equal to 1, whereas the other child particle has a shape factor that is less than unity. Because the parent particle is the same in both cases as is ϕ_1, it is clear that ϕ_w and ϕ_1 do not determine ϕ_2. Therefore, for given values of ϕ_w and ϕ_1, there can be a distribution of values of ϕ_2. As is shown in Figure 2(c), both child particles may have shape factors less than one. This shows that there can be a range of plausible shape factors.

To propose theoretical breakage functions it is first necessary to determine the range of possible values for a child particle's shape factor. In general, any particle's shape factor can range from zero to one. In the case of a child particle, its maximum possible value is one. This is not limited to the case where the parent particle is a cuboid. As shown in Figure 3, it is physically possible with other shapes as well. This is not claiming that it is physically probable; it is just providing a theoretical limit.

The lower limit for the child shape factor can be determined from the parent particle shape factor and the ratio of the child particle volume to the parent particle volume. It is possible that the length, depth, and height of the child particle are the same as those for the parent particle. Because the shape factor used in this work is defined as the ratio of the actual particle volume to the apparent particle volume, and because we know the child particle volume v, the parent particle volume w, and the parent shape factor ϕ_w, the minimum possible child particle shape factor is

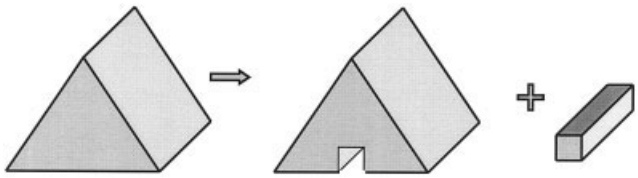

Figure 3. Breakage of a noncuboid into one noncuboid and one cuboid.

$$\phi_{v,\min} = \frac{v\phi_w}{w} \tag{14}$$

where w/ϕ_w is the apparent volume of the parent particle. An example of this can be seen in Figure 4. Again, this shape factor may not be physically probable, but it does provide a minimum limit on the particle shape factor.

The next consideration is the functional form of the breakage distribution function to include the shape factor. When only particle size is considered, the breakage function is written as $b'_v(v, w)$. In this case the second child particle volume is not given because it can be calculated from v and w using Eq. 13. To account for particle shape and to determine exchangeability, the breakage distribution function is expressed as the joint probability $b_\phi(v, \phi_1, \phi_2, w, \phi_w)$. This form lists all of the shape factors, because none of the shape factors can be calculated from the others. Exchangeability can be shown as follows:

$$b_\phi(v_1, \phi_1, \phi_2, w, \phi_w) = b_\phi(v_2, \phi_2, \phi_1, w, \phi_w) \tag{15}$$

In other words, it does not matter which particle volume and shape factor are entered first; the value of the breakage distribution function is the same.

This new functional form is related to the traditional functional form as follows:

$$b'_v(v, w) = \int_0^1 \int_{v_1\phi_w/w}^1 \int_{v_2\phi_w/w}^1 b_\phi(v_1, \phi_1, \phi_2, w, \phi_w) d\phi_2 d\phi_1 d\phi_w \tag{16}$$

Figure 4. Parent particle and child particle with the same length, width, and depth but different shape factors.

As stated earlier, particles cannot be formed below the minimum shape factor. Therefore, $b_\phi(v, \phi_1, \phi_2, w, \phi_w)$ is zero when ϕ_1 is less than $\phi_{1,\min}$ or ϕ_2 is less than $\phi_{2,\min}$.

In the breakage equation given in Eq. 11, the breakage is of the form $b_\phi(v, \phi_1, w, \phi_w)$. The function $b'_\phi(v, \phi_1, \phi_2, w, \phi_w)$ reduces to function $b'_\phi(v, \phi_1, w, \phi_w)$ by integration.

$$b'_\phi(v, \phi_1, w, \phi_w) = \int_{v_2\phi_w/w}^{1} b_\phi(v, \phi_1, \phi_2, w, \phi_w)d\phi_2 \qquad (17)$$

The expression $b'_\phi(v, \phi_1, w, \phi_w)$ indicates the number of particles of size v and shape ϕ_1 formed per particle of size w and shape ϕ_w broken.

The joint distribution function can be written a number of ways. In the most general form, it can be written as

$$b_\phi(v, \phi_1, \phi_2, w, \phi_w) = \frac{A_\phi[f(v_1, \phi_1, w, \phi_w) \otimes f(v_2, \phi_2, w, \phi_w)]}{g(w, \phi_w)} \qquad (18)$$

where A_ϕ is a constant, f is a function of a child particle volume and its shape factor as well as the parent particle volume and its shape factor, and g is a function of the parent particle volume and its shape factor. The symbol $\otimes$ is used to indicate that the operation between the two functions can be addition or multiplication. This breakage distribution function guarantees exchangeability because the function $f(v_i, \phi_i)$ is the same for each child particle. Furthermore, mass conservation is guaranteed if the breakage function meets the following constraint:

$$\int_0^w \int_{\phi_{1,\min}}^1 \int_{\phi_{2,\min}}^1 \frac{v}{w} b_\phi(v, \phi_1, \phi_2, w, \phi_w)d\phi_2 d\phi_1 dv = 1 \qquad (19)$$

This basically states that for each parent particle, the sum of the masses of each of the child particles must equal the total mass of the parent particle. The second constraint for binary breakage is that two child particles are formed from each particle that breaks. This may be written as

$$\int_0^w \int_{\phi_{1,\min}}^1 \int_{\phi_{2,\min}}^1 b_\phi(v, \phi_1, \phi_2, w, \phi_w)d\phi_2 d\phi_1 dv = 2 \qquad (20)$$

This expression guarantees that two child particles are formed from each parent particle for all parent particle shape factors.

The distribution function $b_\phi(v, \phi_1, \phi_2, w, \phi_w)$ can be decomposed to simplify the problem. Specifically, it can be expressed as the product of two types of functions, as shown by

$$b_\phi(v, \phi_1, \phi_2, w, \phi_w) = b'_v(v, w)b_s(\phi_1; v_1, w, \phi_w)b_s(\phi_2; v_2, w, \phi_w) \qquad (21)$$

The first function, $b'_v(v, w)$, is a probability function that gives the probability of producing a particle of volume v given a parent particle of volume w. The second function is a conditional probability, $b_s(\phi_i; v_i, w, \phi_w)$, which yields the probability of forming a particle with a shape factor ϕ_i given that a child particle of volume v_i is formed from a parent particle of volume w and shape factor ϕ_w. For this case, the constraints for mass conservation and binary breakage given in Eqs. 19 and 20 can be rewritten in terms of $b'_v(v, w)$ and $b_s(\phi_i; v_i, w, \phi_w)$. The mass constraint is

$$\int_0^w \frac{v}{w} b'_v(v, w) \int_{\phi_{1,\min}}^1 b_s(\phi_1; v_1, w, \phi_w)d\phi_1 \times \int_{\phi_{2,\min}}^1 b_s(\phi_2; v_2, w, \phi_w)d\phi_2 dv = 1 \qquad (22)$$

and the binary breakage constraint is

$$\int_0^w b'_v(v, w) \int_{\phi_{1,\min}}^1 b_s(\phi_1; v_1, w, \phi_w)d\phi_1 \times \int_{\phi_{2,\min}}^1 b_s(\phi_2; v_2, w, \phi_w)d\phi_2 dv = 2 \qquad (23)$$

The third constraint is exchangeability. This states that the order in which particles are entered into the function does not change the value of the function. The breakage distribution functions developed using Eq. 21 are a subset of the family of functions described by Eq. 18. The following development will focus on the ones described by Eq. 21.

As discussed previously, a family of functions has been developed for $b'_v(v, w)$ to meet the mass conservation, number, and exchangeability constraints (Hill and Ng, 1996). One example of this for binary breakage is the product function with a power-law form given in Eq. 4. For $p = 2$

$$b'_v(v_1, w) = \frac{2(2m + 1)!v_1^m v_2^m}{(m!)^2 w^{2m+1}} \qquad (24)$$

where m is a nonnegative integer. For the case where $m = 0$, the breakage function is

$$b'_v(v_1, w) = \frac{2}{w} \qquad (25)$$

The previous two equations hold true for cases where particle shape is not considered. However, the breakage function $b_\phi(v, \phi_1, \phi_2, w, \phi_w)$ reduces to $b'_v(v, w)$ by Eq. 16. Therefore, Eq. 21 can be used as a basis for developing a new breakage function that incorporates shape.

To meet these constraints, the breakage distribution function can be of the following general form:

$$b_\phi(v_1, \phi_1, \phi_2, w, \phi_w) = \frac{A[f(v_1) \otimes f(v_2)]b_s(\phi_1, v_1, w, \phi_w)b_s(\phi_2, v_2, w, \phi_w)}{g(w)} \qquad (26)$$

where A is a constant, f and g are functions of particle volume, b_s is the shape factor distribution, and $\otimes$ is an operator such as multiplication or addition. Because the constant A along with the functions $f(v_i)$ and $g(w)$ have previously been discussed by Hill and Ng (1996), the remaining discussion will focus on possible functional forms for $b_s(\phi_i; v_i, w, \phi_w)$.

One constraint on the shape distribution function $b_s(\phi_i; v_i, w, \phi_w)$ is that it must be defined over the theoretical limits of ϕ_i.

$$\phi_{\min} \le \phi_i \le \phi_{\max} \tag{27}$$

Another constraint is that it must be defined so that

$$\int_{\phi_{\min}}^{\phi_{\max}} b_s(\phi_i; v_i, w, \phi_w) d\phi_i = 1 \tag{28}$$

In this expression, integration takes place only over the possible values of ϕ_i. If we assume the value of $\phi_{\min}$ given in Eq. 14 and that the maximum shape factor $\phi_{\max} = 1$, then we have the following relations:

$$\frac{v_i \phi_w}{w} \le \phi_i \le 1 \tag{29}$$

$$\int_{v_i\phi_w/w}^{1} b_s(\phi_i; v_i, w, \phi_w) d\phi_i = 1 \tag{30}$$

The limits for the volumetric shape factor given in Eq. 29 apply only to the shape factor defined in Eq. 12. If other shape factors are used, the limits may be different. For illustration purposes Eqs. 29 and 30 will be used in this article. However, if other estimates of $\phi_{\min}$ and $\phi_{\max}$ are used, then the general equations, Eqs. 27 and 28, are applicable.

This functional form of $b_s(\phi_i; v_i, w, \phi_w)$ can be combined with the power-law form of the product function given in Eq. 24, as follows:

$$b_\phi(v_1, \phi_1, \phi_2, w, \phi_w) = \begin{cases} \dfrac{2(2m+1) v_1^m v_2^m b_s(\phi_1; v_1, w, \phi_w) b_s(\phi_2; v_2, w, \phi_w)}{(m!)^2 w^{2m+1}} & \text{for } \begin{cases} \dfrac{v_1\phi_w}{w} \le \phi_1 \le 1 \\ \text{and} \\ \dfrac{v_2\phi_w}{w} \le \phi_2 \le 1 \end{cases} \\ 0 & \text{for } \begin{cases} \phi_1 < \dfrac{v_1\phi_w}{w} \\ \text{or} \\ \phi_2 < \dfrac{v_2\phi_w}{w} \end{cases} \end{cases} \tag{31}$$

For the summation form of the breakage distribution function given in Eqs. 6, 7, and 8, the expression is

$$b_\phi(v_1, \phi_1, \phi_2, w, \phi_w) = \begin{cases} \dfrac{(m+1)(v_1^m + v_2^m) b_s(\phi_1; v_1, w, \phi_w) b_s(\phi_2; v_2, w, \phi_w)}{w^{m+1}} & \text{for } \begin{cases} \dfrac{v_1\phi_w}{w} \le \phi_1 \le 1 \\ \text{and} \\ \dfrac{v_2\phi_w}{w} \le \phi_2 \le 1 \end{cases} \\ 0 & \text{for } \begin{cases} \phi_1 < \dfrac{v_1\phi_w}{w} \\ \text{or} \\ \phi_2 < \dfrac{v_2\phi_w}{w} \end{cases} \end{cases} \tag{32}$$

Both Eqs. 31 and 32 are general forms of the equation for the binary breakage case where m is a nonnegative integer. The key idea is to substitute an appropriate shape factor function, $b_s(\phi_i; v_i, w, \phi_w)$, into these equations.

Uniform Shape Distribution. One of the simplest models would be to assume that the particles are evenly distributed across a shape factor range at a given particle size. Let us assume that $b_s(\phi_i;\, v_i,\, w,\, \phi_w)$ is of the following form:

$$b_s(\phi_i;\, v_i,\, w,\, \phi_w) = \frac{1}{1 - \dfrac{v_i\phi_w}{w}} \tag{33}$$

It can be shown that this expression meets the constraint given in Eq. 30. If this is combined with a product-law function with a power-law form, the resulting breakage function is

$$b_\phi(v_1,\, \phi_1,\, \phi_2,\, w,\, \phi_w) = \begin{cases} \dfrac{2(2m+1)v_1^m v_2^m}{(m!)^2 w^{2m+1}\left(1 - \dfrac{v_1\phi_w}{w}\right)\left(1 - \dfrac{v_2\phi_w}{w}\right)} & \text{for } \begin{cases} \dfrac{v_1\phi_w}{w} \le \phi_1 \le 1 \\ \text{and} \\ \dfrac{v_2\phi_w}{w} \le \phi_2 \le 1 \end{cases} \\ 0 & \text{for } \begin{cases} \phi_1 < \dfrac{v_1\phi_w}{w} \\ \text{or} \\ \phi_2 < \dfrac{v_2\phi_w}{w} \end{cases} \end{cases} \tag{34}$$

For the summation function with a power-law form, the resulting breakage function is

$$b_\phi(v_1,\, \phi_1,\, \phi_2,\, w,\, \phi_w) = \begin{cases} \dfrac{(m+1)(v_1^m + v_2^m)}{w^{m+1}\left(1 - \dfrac{v_1\phi_w}{w}\right)\left(1 - \dfrac{v_2\phi_w}{w}\right)} & \text{for } \begin{cases} \dfrac{v_1\phi_w}{w} \le \phi_1 \le 1 \\ \text{and} \\ \dfrac{v_2\phi_w}{w} \le \phi_2 \le 1 \end{cases} \\ 0 & \text{for } \begin{cases} \phi_1 < \dfrac{v_1\phi_w}{w} \\ \text{or} \\ \phi_2 < \dfrac{v_2\phi_w}{w} \end{cases} \end{cases} \tag{35}$$

In both Eqs. 34 and 35, m is a nonnegative integer. Both functional forms meet the constraints for exchangeability, mass conservation, and the production of two child particles.

Parabolic Shape Distribution. It seems physically unrealistic that out of the possible shapes produced the resulting child particle would be a perfect cuboid or have the minimum shape factor. A more realistic distribution might be a parabolic distribution where most child particles have shape factors in the middle of the range. The parabolic shape distribution can assume the following functional form:

$$b_s(\phi_i;\, v_i,\, w,\, \phi_w) = \left[(1 - \phi_i)\left(\frac{v_i\phi_w}{w} - \phi_i\right)\right] \Big/ C_i \tag{36}$$

where

$$C_i = \frac{1}{6}\left(\frac{v_i\phi_w}{w}\right)^3 - \frac{1}{2}\left(\frac{v_i\phi_w}{w}\right)^2 + \frac{1}{2}\frac{v_i\phi_w}{w} - \frac{1}{6} \tag{37}$$

and where i indicates which particle is under consideration. For each particle volume v_i, this function yields a parabolic distribution of shape factors such that the breakage distribution function has the value of zero at shape factors of 1 and $v_i\phi_w/w$. The maximum value of the breakage distribution function is halfway between these two shape factors. The function given in Eqs. 36 and 37 meets the constraint given in Eq. 30.

The parabolic shape function should be able to model a range of shapes from opening downward as given above or opening upward with a minimum value of zero. All shape factors must be greater than or equal to zero between $\phi_{\min}$ and $\phi_{\max}$. A more general form that allows this is

$$b_s(\phi_i;\, v_i,\, w,\, \phi_w) = \left[z_i\left(\phi_i - \frac{1}{2} - \frac{v_i\phi_w}{2w}\right)^2 + k_i\right] \Big/ C_i \tag{38}$$

where

$$C_i = k_i\left(1 - \frac{v_i\phi_w}{w}\right) + z_i\left[\frac{1}{12} - \frac{1}{4}\frac{v_i\phi_w}{w} + \frac{1}{4}\left(\frac{v_i\phi_w}{w}\right)^2 - \frac{1}{12}\left(\frac{v_i\phi_w}{w}\right)^3\right] \tag{39}$$

and where z_i and k_i are constants or functions of v_i, w, and ϕ_w. For all nonzero values of z_i and for k_i defined as

$$k_i = -\frac{z_i}{4}\left(1 - \frac{v_i\phi_w}{w}\right)^2 \tag{40}$$

the curves are the same as those obtained by Eqs. 36 and 37.

Other Shape Distributions. Other functions are possible for $b_s(\phi_i;\, v_i,\, w,\, \phi_w)$. The only requirements are that they meet the constraint given in Eq. 30 and that they have nonnegative values over the shape factor range of interest. Some functions that meet these constraints are listed in Table 2. These functions can be the exponential function as shown in Eq. 41, the Dirac delta function given in Eq. 42, where ϕ_0 is the only shape factor that is produced, or the decreasing line given in Eq. 43. One characteristic of the exponential function given in Eq. 41 is that it can be adjusted by varying the value of $\kappa(w)$ to control the steepness of the exponential curve.

Multiple particle breakage

The same concepts can be extended to multiple particle breakage. In this case, the concern is to produce a function where a parent particle of volume w and shape factor ϕ_w produces p particles of various volumes and shape factors. Because the sum of the volumes of the child particles must

Table 2. Shape Factor Functions

Description	$b_s(\phi_i;\ v_i,\ w,\ \phi_w)$	Eq.
Uniform	$b_s(\phi_i; v_i, w, \phi_w) = \dfrac{1}{1 - \dfrac{v_i\phi_w}{w}}$	33
Parabolic	$b_s(\phi_i; v_i, w, \phi_w) = \left[z\left(\phi_i - \dfrac{1}{2} - \dfrac{v_i\phi_w}{2w}\right) + k_i\right]\Big/ C_i$	38
	$C_i = k_i\left(1 + \dfrac{v_i\phi_w}{w}\right) + z\left[\dfrac{1}{12} - \dfrac{1}{4}\dfrac{v_i\phi_w}{w} + \dfrac{1}{4}\left(\dfrac{v_i\phi_w}{w}\right)^2 - \dfrac{1}{12}\left(\dfrac{v_i\phi_w}{w}\right)^3\right]$	39
Exponential	$b_s(\phi_i;\ v_i,\ w,\ \phi_w) = \kappa(w)e^{\kappa(w)\phi_i}/(e^{\kappa(w)} - e^{\kappa(w)v_i\phi_w/w})$	41
Dirac Delta	$b_s(\phi_i;\ v_i,\ w,\ \phi_w) = \delta(\phi - \phi_0)$	42
Decreasing Line	$b_s(\phi_i; v_i, w, \phi_w) = (1 - \phi)\Big/\left[\dfrac{1}{2} - \dfrac{v_i\phi_w}{w} + \dfrac{1}{2}\left(\dfrac{v_i\phi_w}{w}\right)^2\right]$	43

equal the original parent particle volume, the following relation is available:

$$w = \sum_{i=1}^{p} v_i \tag{44}$$

From this relation, it is clear that the volume of particle p is

$$v_p = w - \sum_{i=1}^{p-1} v_i \tag{45}$$

Therefore, the breakage function can be written as a joint probability without explicitly listing v_p as $b_\phi(v_1, v_2, v_3, \ldots, v_{p-1};\ \phi_1, \phi_2, \phi_3, \ldots, \phi_p;\ w, \phi_w)$. Again, it is necessary to list the shape factor of each particle since specifying one shape factor does not specify the other shape factors. The reasoning for this is the same as it was for binary breakage. Also, the limits on shape factor values given in Eq. 29 still apply.

This joint probability is reduced to a marginal probability by integration:

$$b'(v_1, w) = \int_0^{w-v_1}\int_0^{w-v_1-v_2}\cdots\int_0^{w-\sum_{i=1}^{p-2} v_i}\int_0^1\int_{v_1\phi_w/w}^1 \times \int_{v_2\phi_w/w}^1\cdots\int_{v_p\phi_w/w}^1 b_\phi(v_1, v_2, v_3, \ldots, v_{p-1};\ \phi_1, \phi_2, \phi_3, \ldots, \phi_p;\ w, \phi_w)d\phi_p d\phi_{p-1}\cdots d\phi_2 d\phi_1 d\phi_w dv_{p-1}\cdots dv_3 dv_2 \tag{46}$$

The section on binary breakage showed that the values of the shape factors of child particles could range from $v_1\phi_w/w$ to 1. Because this is still true for multiple particle breakage, this is the range of integration given for each shape factor. To include particle shape in population balances including the shape factor, the following form is more useful:

$$b'_\phi(v_1, \phi_1, w, \phi_w) = \int_0^{w-v_1}\int_0^{w-v_1-v_2}\cdots\int_0^{w-\sum_{i=1}^{p-2} v_i} \int_{v_2\phi_w/w}^1\cdots\int_{v_p\phi_w/w}^1 b_\phi(v_1, v_2, v_3, \ldots, v_{p-1};\ \phi_1, \phi_2, \phi_3, \ldots, \phi_p;\ w, \phi_w)d\phi_p d\phi_{p-1}\cdots d\phi_2 dv_{p-1}\cdots dv_3 dv_2 \tag{47}$$

The same constraints exist for multiple particle breakage distribution functions. If p particles are produced when a parent particle breaks, then the following constraint must be met:

$$\int_0^w\int_0^1 b'_\phi(v, \phi_1, w, \phi_w)d\phi_1 dv = p \tag{48}$$

The mass conservation constraint is

$$\int_0^w\int_0^1 \frac{v}{w} b'_\phi(v, \phi_1, w, \phi_w)d\phi_1 dv = 1 \tag{49}$$

The expression for $b'_\phi(v_1, \phi_1, w, \phi_w)$ given in Eq. 47 is substituted in both Eqs. 48 and 49.

To include shape factor with the product distribution function with a power-law form, as stated in Eq. 4, the functional form of the joint breakage distribution function is

$$b_\phi(v_1, v_2, \ldots, v_{p-1};\ \phi_1, \phi_2, \ldots, \phi_p;\ w, \phi_w) = \frac{p[m + (m+1)(p-1)]!}{(m!)^p} \times \frac{(\prod_{i=1}^{p-1} v_i^m)(w - \sum_{i=1}^{p-1} v_i)^m(\prod_{i=1}^{p} b_s(\phi_i; v_i, w, \phi_w))}{w^{pm+p-1}} \tag{50}$$

After integrating over the shape factors of all the child particles, Eq. 50 reduces to Eq. 4. This equation can also be simplified using Eq. 47 to yield

$$b'_\phi(v,\ \phi_v,\ w,\ \phi_w) = \frac{p v^m (w - v)^{m+(m+1)(p-2)}[m + (m+1)(p-1)]! b_s(\phi_i;\ v_i,\ w,\ \phi_w)}{w^{pm+p-1} m![m + (m+1)(p-2)]!} \tag{51}$$

This same approach can be taken with the power-law form of the summation function to yield

$$b_\phi(v_1,\ v_2,\ \ldots,\ v_{p-1};\ \phi_1,\ \phi_2,\ \ldots,\ \phi_p;\ w,\ \phi_w) = \frac{A_{m,p}[\sum_{i=1}^{p-1} v_i^m + (w - \sum_{i=1}^{p-1} v_i)^m]([\prod_{i=1}^{p} b_s(\phi_i;\ v_i,\ w,\ \phi_w))}{w^{m+p-1}} \tag{52}$$

where $A_{m,p}$ is given in Eqs. 7 and 8. For $p = 2$, the above expressions can be simplified to

$$b'_\phi(v,\ \phi_v,\ w,\ \phi_w) = \frac{(m+1)}{w^{m+1}}[v^m + (w - v)^m] b_s(\phi_i;\ v_i,\ w,\ \phi_w) \tag{53}$$

For $p > 2$, the expression is

$$b'_\phi(v,\ \phi_v,\ w,\ \phi_w) = \frac{A_{m,p}\left[v^m (w - v)^{p-2}\left(\prod_{i=0}^{p-3} \frac{1}{i+1}\right) + (w - v)^{m+p-2}\left(\frac{p-1}{A_{m,p-1}}\right)\right] b_s(\phi_i;\ v_i,\ w,\ \phi_w)}{w^{m+p-1}} \tag{54}$$

For both the product and summation functions, the shape factor distribution $b_s(\phi_i;\ v_i,\ w,\ \phi_w)$ can be the uniform distribution given in Eq. 33, the parabola distribution given in Eqs. 38 and 39, or any other shape distribution that yields nonnegative values in the range of interest and meets the criteria given in Eqs. 29 and 30.

Results

Let us now examine some of these breakage functions graphically. An examination of the breakage distribution functions indicates that if we take $b'_\phi(v_1,\ \phi_1,\ w,\ \phi_w)$ for the product function with a power-law form and multiply it by w, we get a general function written in terms of v/w. For example, for binary breakage ($p = 2$) and $m = 1$ we have

$$b'_\phi(v,\ \phi_v,\ w,\ \phi_w) = \frac{12 v(w - v) b_s(\phi_i;\ v_i,\ w,\ \phi_w)}{w^3} \tag{55}$$

which goes to

$$w b'_\phi(v,\ \phi_v,\ w,\ \phi_w) = 12\left[\left(\frac{v}{w}\right) - \left(\frac{v}{w}\right)^2\right] b_s(\phi_i;\ v_i,\ w,\ \phi_w) \tag{56}$$

This indicates that the curves are qualitatively the same for all values of w and that w influences only the magnitude of the breakage distribution functions. A similar approach can be taken with the summation function with a power-law form by multiplying $b'_\phi(v_1,\ \phi_1,\ w,\ \phi_w)$ by w to get a general function written in terms of v/w.

To illustrate the effect on the breakage distribution function, calculations were performed for binary breakage using the product function with a power-law form and $m = 1$. Similar results would be obtained if more than two child particles were formed from each breakage.

The shape factor distribution has a strong effect on the resulting breakage distribution function. To illustrate the differences between the shape functions, these comparisons use a parent particle shape factor of 1.0, and a ratio of 0.4 for the child particle to parent particle volume. For the parabolic shape function, Figure 5 shows a range of breakage functions for various of $k_i(v,\ w,\ \phi_w)$. The function $k_i(v,\ w,\ \phi_w)$ given in Eq. 40 gives one limit on the parabola shape. The opposite limit is when k_i is zero. If k_i is zero and z_i is not zero, the curve opens upward and $b_s(\phi_i;\ v_i,\ w,\ \phi_w)$ is equal to zero at the center of the parabola. As k_i approaches ∞ or $-\infty$, the distribution approaches the uniform distribution. To have nonzero values for the breakage distribution function, $k_i(v,\ w,\ \phi_w)$ must not be between zero and the value given in Eq. 40. Other shape factors are possible, as shown in Table 2. Figure 6 shows both the exponential and decreasing line functions as a function of

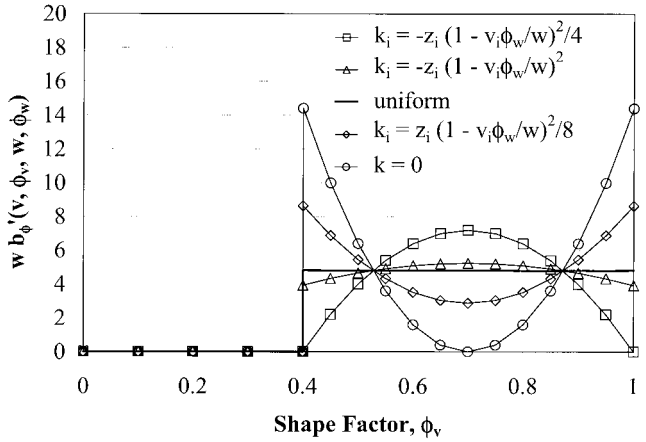

Figure 5. Breakage distribution function using parabolic shape function for binary breakage with v/w = 0.4 and ϕ_w = 1.

shape factor. For the exponential function, the curve approaches the uniform breakage function as the value of $\kappa(w)$ is decreased. As $\kappa(w)$ is increased, the exponential shape function predicts a higher percentage of particles with shape factors near unity.

Even for the same shape function, the relative size of the child particle to the parent particle has a significant effect. In this set of comparisons, the parent particle shape factor is set to 1, the parabolic shape function is used, and k_i is defined by Eq. 40. These curves are shown in Figure 7 for binary breakage with $m = 1$. As set up in the equations, the parabola narrows as v/w approaches 1. Because the number of particles is distributed over a narrower range of shape factors as v/w approaches 1, the maximum value of $b'_\phi(v, \phi_v, w, \phi_w)$ increases as v/w is increased.

The parent particle shape factor also has a strong effect on the breakage function. One example of this is shown in Figure 8 for a parabolic shape factor with v/w set to 0.5 and k_i defined by Eq. 40. The parabola spreads over a wider range of shape factors as ϕ_w is decreased. This is expected since the minimum shape factor $v\phi_w/w$ decreases as ϕ_w is decreased.

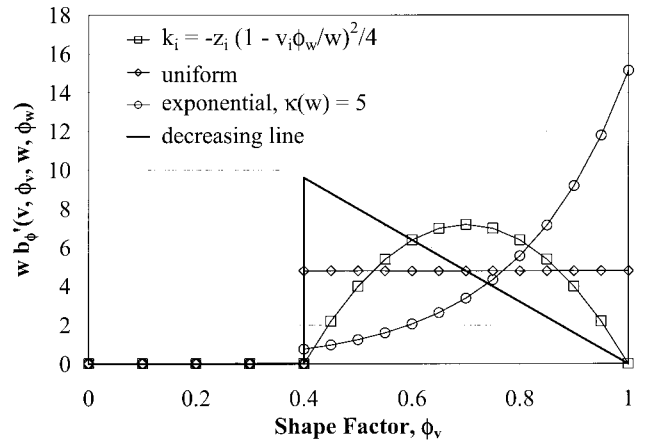

Figure 6. Comparison of breakage distribution functions using different shape functions for binary breakage with v/w = 0.4 and ϕ_w = 1.

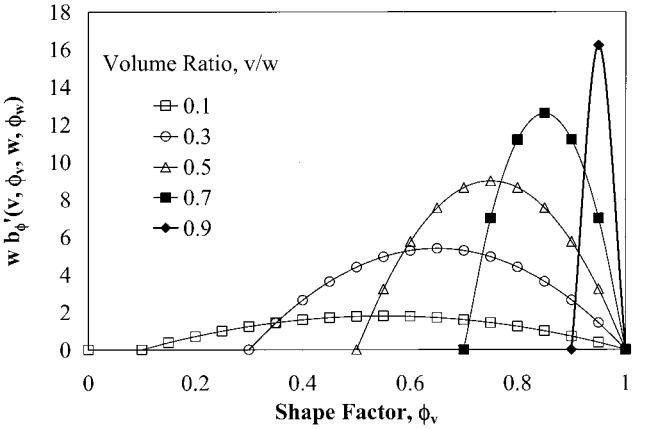

Figure 7. Parabolic shape function for binary breakage with ϕ_w = 1 (product function with a power-law form, m = 1).

Numerical Solution

Method

The breakage equation given in Eq. 11 can be solved by reducing it to a set of discretized equations. The technique used is similar to that described by Hill and Ng (1995, 1996). This method was developed for the case without shape factors, but can easily be extended to include particle shape. In the previous article, the set of discretized equations is given by

$$\frac{dN_i}{dt} = \sum_{j=i+1}^{\infty} \beta_j b_{ij} S_j N_j - \delta_i S_i N_i \tag{57}$$

where N_i is the number of particles in interval i, S_i is the specific rate of breakage in interval i, b_{ij} is the discretized breakage distribution function, and β_j and δ_i are factors for the birth and death terms, respectively. These birth and death term factors guarantee that mass is conserved during breakage and that p particles are produced when a parent particle breaks.

To include particle shape, Eq. 57 is modified to

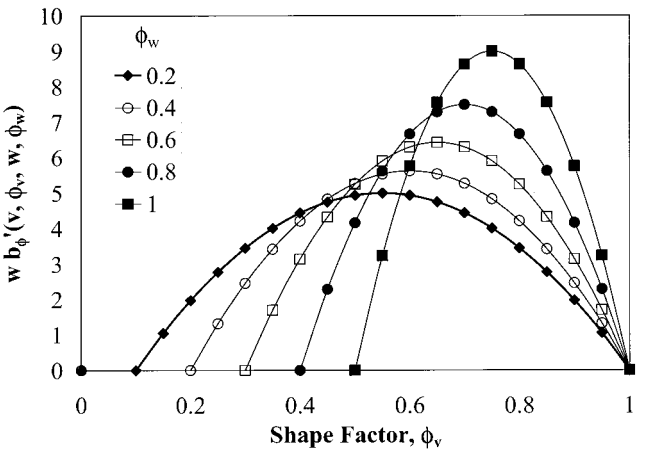

Figure 8. Parabolic shape function for binary breakage with v/w = 0.5 (product function with a power-law form, m = 1).

$$\frac{dN_{\phi,ik}}{dt} = \sum_{j=i}^{\infty} \sum_{l=1}^{l_{\max}} \beta_{\phi,jl} b_{\phi,ikjl} S_{\phi,jl} N_{\phi,jl} - S_{\phi,ik} N_{\phi,ik} \qquad (58)$$

where $N_{\phi,ik}$ is the number of particles in size interval i and shape interval k, $S_{\phi,ik}$ is the specific rate of breakage for particles in size interval i and shape interval k, $\beta_{\phi,ik}$ is the birth term factor for particles broken from size interval i and shape interval k, and the discretized breakage function including shape factor $b_{\phi,ikjl}$ is defined as

$$b_{\phi,ikjl} = \int_{v_{i-1}}^{v_i} b'_v(u, v_j)du \int_{\phi_{k-1}}^{\phi_k} b_s(\phi; v_i, v_j, \phi_l)d\phi \qquad (59)$$

for $\phi_{k-1} > \phi_{\min}$ and is defined as

$$b_{\phi,ikjl} = \int_{v_{i-1}}^{v_i} b'_v(u, v_j)du \int_{\phi_{\min}}^{\phi_k} b_s(\phi; v_i, v_j, \phi_l)d\phi \qquad (60)$$

for $\phi_{k-1} < \phi_{\min} < \phi_k$. It is convenient to use an average value of $\phi_{\min}$ of $v_i\phi_l / v_j$. The discretized breakage distribution factor with shape factor reduces to the discretized breakage function without shape factor as shown

$$b_{ij} = \sum_{l=1}^{n_\phi} \sum_{k=k_{\lim}}^{n_\phi} b_{\phi,ijkl} \qquad (61)$$

where n_ϕ is the number of shape intervals and $k_{\lim}$ is the minimum value of k that corresponds to $\phi_{\min}$. In this case, the birth term factor is calculated as for multiple particles (Hill and Ng, 1996) and the death term factor is omitted. Originally the death term accounted for child particles falling into the same size interval as their parent particles. Here, this is accounted for by using birth terms in the parent particle size interval. Instead of summing from $j = i + 1$ as in Eq. 57, the sum starts at $j = i$. That is, a birth term is being included for particles breaking from interval j to fall into the same interval. The term $b_{i,i}$ is defined as $1 - \delta_i$. In this case, the objective is to show that, although a particle may fall into the same size interval, it may have a different shape factor than the parent particle.

Results

We first need to test the method to show that it conserves mass and correctly predicts the change in the number of particles with time. For the case of binary breakage with a uniform distribution function with $m = 0$, the analytical solution for the mass in each size interval M_i (Hill and Ng, 1995) is given by

$$M_i(t) = R(v_{i-1}, 0)\exp(-S_c t v_{i-1}^2) - R(v_i, 0)\exp(-S_c t v_i^2) \qquad (62)$$

where $R(v, 0)$ is the total mass of particles greater than size v at time zero, S_c is a constant, and

$$S(v) = S_c v^2 \qquad (63)$$

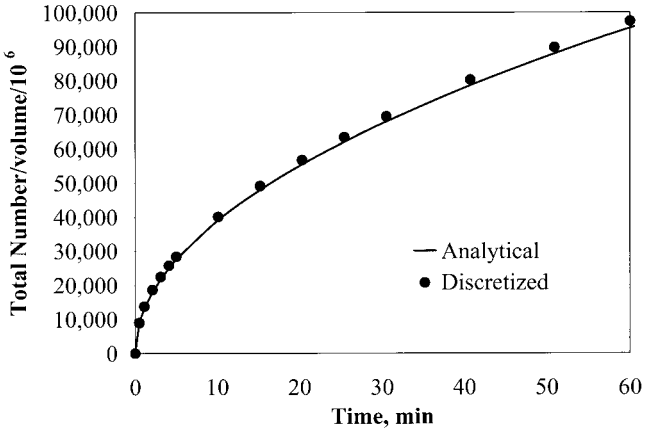

Figure 9. Change in total number of particles with time for uniform breakage function.

is the specific rate of breakage. The analytical solution for the number of particles in each size interval (Hill and Ng, 1995) is given by

$$N_i(t) = \frac{\sqrt{\pi S_c t}}{\rho} M_T[\text{erf}(v_i\sqrt{S_c t}) - \text{erf}(v_{i-1}\sqrt{S_c t})] \qquad (64)$$

where erf is the error function and ρ is the particle density.

For comparison with the analytical solution, the breakage rate constant S_c is set to 5×10^{-12} min^{-1} and the density is set to 3.217 g/cm, which is the density of SiC. To compare with the analytical solution, the specific rate of breakage is set so that is does not depend on the shape factor. Also, the breakage function is set to the binary breakage function with a uniform size distribution. For the discretized simulation, particles in the smallest size interval are not allowed to break. This is based on the idea that below a critical size, particles usually deform instead of breaking (Kendall, 1978). This smallest size interval ranges from 0 to 594.0418 μm^3. Subsequent size intervals are set using a geometric ratio of 2 so that for $i > 1$, $v_i = 2v_{i-1}$. The initial charge to the batch crusher, M_T, is 10 kg of particles evenly distributed with respect to size across the top size interval (1.557 to 3.114×10^8 μm^3). The volumetric shape factor of all the initial particles is set to unity.

The discretized method is compared with the analytical solution to show how the total number of particles changes with time. Figure 9 shows that this discretized method closely approximates the change in the total number of particles. Both the discretized method and the analytical solution conserved the total mass of solids.

Given that the uniform shape distribution is a constant value between the limiting shape factors (as shown in Figure 6), one might expect the shape distribution of a given particle size to have a constant value. However, this is not always the case. Figure 10(a) shows the shape distribution for selected average particle volumes as calculated by the discretized method. These are results generated after 0.5 min of breakage. The total number of particles in the size–shape intervals are plotted at the maximum value of a shape interval. Although particles with an average particle volume of $\leq$57,028 μm^3 exhibit an almost constant shape factor distribution, particles with an average

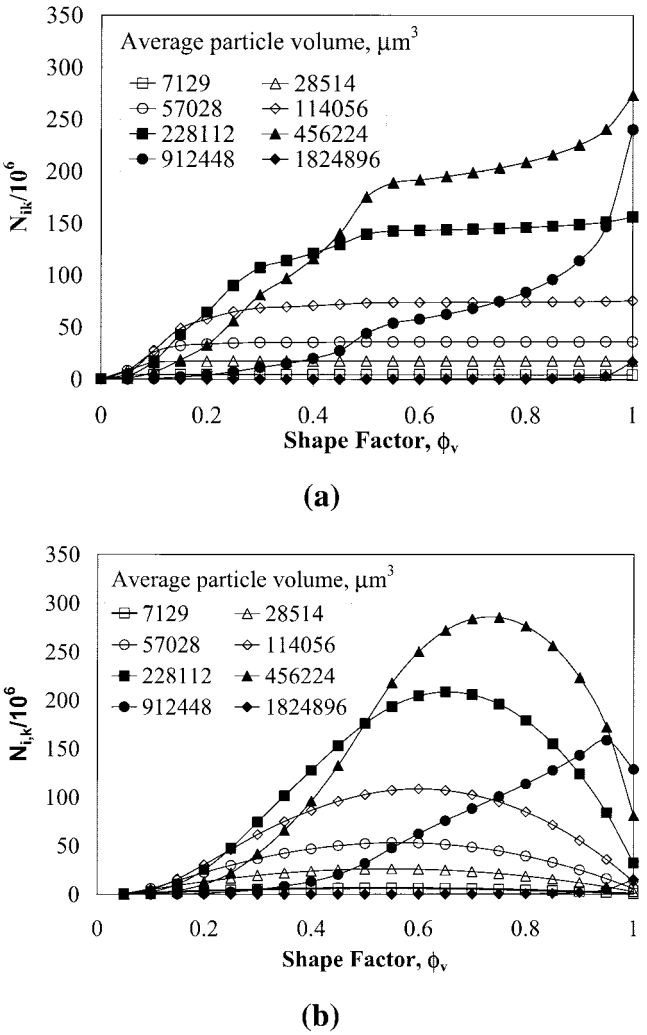

Figure 10. Shape factor distributions for selected particle sizes after 0.5 min of breakage for a uniform breakage function: (a) uniform shape distribution; (b) parabolic shape distribution.

size of $\geq$228,112 μm^3 are far from a constant shape factor distribution. This may be explained by recalling that this shape distribution is formed from a sequence of breakage steps, and that there is a lower limit on the child particle shape factor that depends on the characteristics of the parent particle.

For example, one set of parent particles of size w_1 will break and form child particles of size v with shape factors ranging from 0.5 to 1. A second set of parent particles of size w_2 will break and form child particles of size v with shape factors ranging from 0.3 to 1. Although all of the breakage is governed by a uniform shape factor, the resulting shape distribution at size v is not uniform because the two resulting distributions are added.

A second set of simulations was performed using a parabolic shape distribution function with k_i set by Eq. 40. For this set of simulations, mass is conserved and the change in the total number of particles is identical to the results shown in Figure 9.

Shape distribution results are shown in Figure 10(b), where the breakage distribution function has a shape function with a parabolic form. Here, particles with an average volume of $\leq$228,112 μm^3 have a roughly parabolic shape distribution, whereas particles with an average volume of 912,448 μm^3 do not exhibit a parabolic form to the shape distribution. For the smaller particle sizes, the resulting particle shape factor distribution for the parabolic shape distribution is distinguishable from the shape factor distribution generated using the uniform shape function.

One might expect these shape distributions to change as grinding continues because the results of many parent particles breaking would overlap. The results of 60 min of breakage are shown in Figure 11(a) and (b) for the uniform shape distribution and the parabolic shape distribution, respectively. There is a distinct difference in the results of these two sets of shape distributions. As expected, the particle sizes are smaller after 60 min of grinding, although the general trends shown after 0.5 min of grinding still appear. In Figure 11(a), particles with an average particle volume of $\leq$14,257 μm^3 exhibit an almost constant shape factor distribution, whereas larger particles do

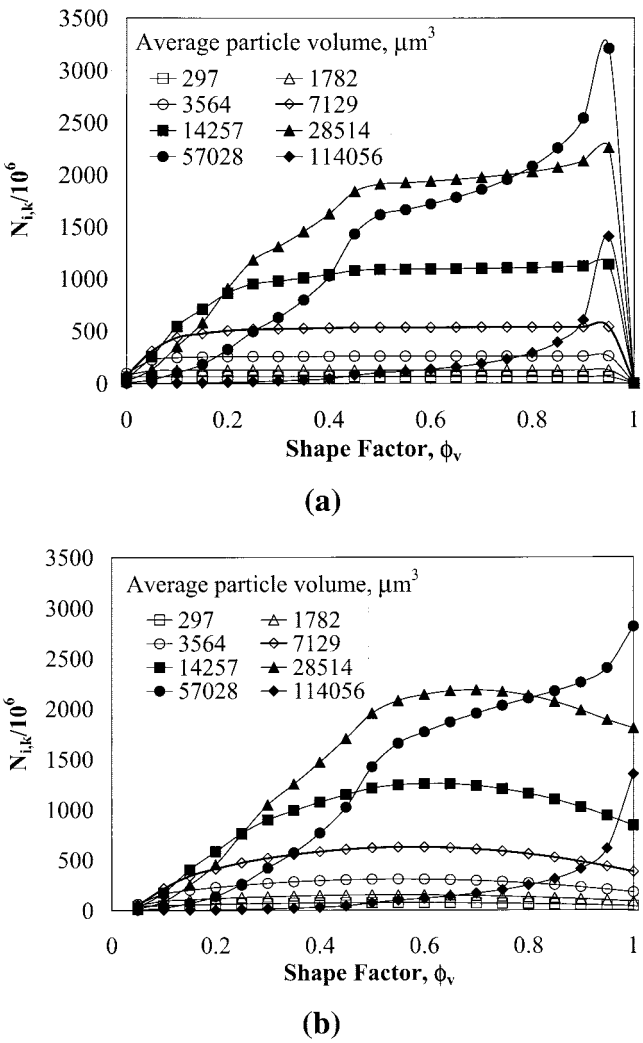

Figure 11. Shape factor distributions for selected particle sizes after 60 min of breakage for a uniform breakage function: (a) uniform shape distribution; (b) parabolic shape distribution.

not. In Figure 11(b), particles with an average particle volume of $\leq$14,257 μm^3 exhibit an almost parabolic shape factor distribution, whereas larger particles do not.

Comparison with Empirical Results

Work by Mazzarotta et al. (1996) on sugar crystals indicates that the crystals become more rounded with time. Sugar crystals are very close to being cubes. These researchers state that the initial roundness of the samples is 1.28, which is essentially the same as the roundness of a cube (1.273). The volumetric shape factor of a cube is 1.0, whereas that of a sphere is 0.524. Therefore if the sugar crystals become more rounded, the volume shape factor should decrease from 1.0 toward 0.524. Any of the breakage distribution functions in Figures 5 and 6 will produce more roundness. In fact, this is what is shown in the simulation results in Figures 10(a) and (b), and 11(a) and (b). This indicates that the proposed functions are qualitatively plausible.

To determine whether the theoretical functions can adequately represent real systems, it is necessary to quantitatively compare the theoretical results with empirical data from real systems. One difficulty with comparisons is that different shape factors give different information about the particle system. Knowing one set of shape factor data does not necessarily provide enough information to determine other shape factors.

For example, researchers (Mazzarotta et al. 1996) have reported the average roundness as a function of breakage time. However, the shape factor used in the PBEs is the ratio of the actual particle volume to the product of the product lengths in the x, y, and z directions. A particle with a roundness of 1.3 could be a cuboid with a volume shape factor of 1.0 or an ellipsoid with a volume shape factor of $\pi/6$. That is, there is not a one-to-one correspondence between roundness and the volume shape factor. There are similar problems using the aspect ratio to predict particle volume.

A better estimate of the volume shape factor can be obtained if at least two shape factors are available. For example, a cuboid with a roundness of 1.3 could have dimensions of 7.5, 10, and 7.5 microns and an aspect ratio of 1.3333, whereas an ellipsoid with a roundness of 1.3 could have dimensions of 4.7, 4.7, and 10 microns and an aspect ratio of 2.13. Although the roundness of each particle is the same, the aspect ratios are quite different.

This information is available for poly(vinyl acetate) particles broken in a mill (Molina-Boisseau et al., 2002). The initial charge to the mill is a bimodal distribution with a main peak near 95 μm and a small peak at 0.5 μm. The average particle size, d_{50}, and average values of shape descriptors are reported as a function of the grinding time. The aspect ratios and the roundness values are used to estimate average volume shape factors at various grinding times. All averaging is done on a volume basis.

For simulation, an initial charge of 10 kg of particles was distributed so that 2 mass percent of the particles are uniformly distributed from 0 to 1 microns. The remaining 98 mass percent of the particles are uniformly distributed from 80 to 101.6 μm. A breakage rate of $5 \times 10^{-9}\, v^{1.35}\ \text{min}^{-1}$ is used, where v is the particle volume in μm^3. The functional form of the breakage distribution function is the product function with a power-law form where seven child particles are formed from each parent

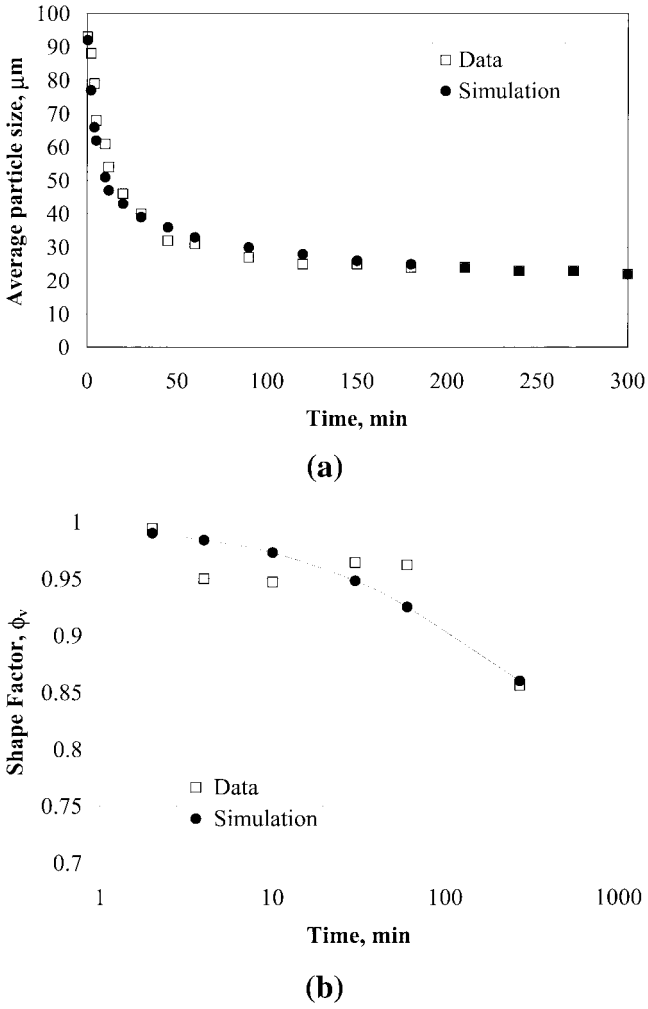

Figure 12. Comparison of simulation results with experimental data: (a) average particle size; (b) average volumetric shape factor.

particle and the power-law exponent is 1. A comparison of the average particle sizes of the simulation against the data is shown in Figure 12(a). The exponential function (Eq. 41) was chosen for the shape distribution function because most of the child particles formed have shape factors near unity, like the experimental data. For simulation, the value $\kappa(w)$ was varied as a function of the parent particle size according to the following expression

$$\kappa(w) = 30\left(\frac{w}{1.049 \times 10^6}\right)^{0.6} \tag{65}$$

where w is in μm^3. This functional form for $\kappa(w)$ was used because it fit the data much better than using a constant value for $\kappa(w)$.

To compare the data with the simulation results, the volume shape factor was estimated using the average aspect ratio and average roundness data. Although this estimation is not exact, it should compare well with the actual data. For example, it is clear from the data that the broken particles are not spheres. As shown in Figure 12(b), the simulation results compared well

with the experimental data. For all points the difference between the simulation results and the data is less than 4%. This demonstrates that these theoretical shape factors can represent actual data.

Concluding Remarks

Accounting for changes in particle size and shape attributed to breakage is difficult because of the irregularity of the resulting particle shapes. There is often a significant difference between the actual particle volume and the apparent volume given by the length, height, and width of the particle. One approach is to introduce a shape factor. In most studies, researchers assume a constant shape factor. However, early work by Dalla Valle and Goldman (1939) tests this assumption that there is a constant shape factor and shows that the shape factor varies for crushed quartz particles in different size ranges. Recent work by Lohmander (2000a) states that using a median value of the shape factor does not give enough information; it is necessary to know the shape factor distribution. It is clear that shape factor distributions need to be included in particulate breakage modeling. To meet this need, the objective of this research is to provide a technique for modeling changes in both the size and shape factor distributions attributed to particle breakage. This requires the development of appropriate breakage distribution functions.

A method is presented for developing breakage distribution functions that incorporate both particle size and shape. These functions ensure that mass is conserved, allow the user to choose how many particles will be formed from parent particle breakage, and allow the user to choose the shape distribution of particles at a given particle size. This method is demonstrated for a set of shape distribution functions including both uniform and parabolic shape distributions. Although a variety of shape distribution functions are presented, researchers are not limited to this set. Additional shape distribution functions can be generated using the given procedure to meet the required constraints.

A discretized solution technique for the breakage equation with shape factor is also developed. Simulation results compared with the analytical solution show that the discretized solution method correctly predicts changes in the total number of particles and conserves mass. A comparison of particles with uniform shape factor breakage functions to particles with parabolic shape factor breakage functions indicates that the resulting particles can have distinguishable shape factor distributions. Comparison of simulation results with experimental data show that changes in particle shape can be adequately modeled by using the proposed theoretical breakage functions.

Although this method provides a basis for creating breakage distribution functions, it has not tried to solve the inversion problem where empirical breakage distribution functions are determined from the data. Ramkrishna (2000) presents an overview of much of the research on the inversion problem. Previous work in this area accounts for the PSD (Sathyagal et al., 1995) but not the shape factor distribution. Given the added complexity of adding particle shape, this is a challenging problem. Ramkrishna and Mahoney (2002) discuss the problem of inverting multidimensional PBEs. Although they do not address particle breakage, they do provide a starting point for further research.

This method can be made more general. That is, it is usually desirable to know more than just the particle volume and the shape factor to characterize the particle shape. One could write a breakage equation in terms of v, $L_{v,x}$, $L_{v,y}$, and ϕ_v, where the subscript v indicates that this is a parameter of a particle of volume v. Using Eq. 12, $L_{v,z}$ can be determined from the other variables. If particle lengths are used, it is necessary to use more than one length for irregular shaped particles. For spheres and cubes a characteristic particle length would be adequate, although a single particle length would not describe needle or plate shaped particles. Clearly, much research remains to be done in determining the statistics of multiple particle breakage, including particle shape.

Acknowledgments

This material is based upon work supported by the National Science Foundation under Grant No. 0225700.

Literature Cited

Allen, T., *Particle Size Measurement*, 2nd Edition, Chapman & Hall, London (1975).

Bravi, M., S. DiCave, and B. Mazzarotta, "Attrition Behaviour of Different Crystals in Stirred Vessels at Just Off-bottom Suspension Conditions," *Proc. 14th Int. Symp. Ind. Cryst.*, Inst. of Chemical Engineers, Rugby, UK, pp. 1341–1351 (1999).

Buffham, B. A., "The Size and Compactness of Particles of Arbitrary Shape: Application to Catalyst Effectiveness Factors," *Chem. Eng. Sci.*, **55**, 5803 (2000).

Conti, R., and A. W. Nienow, "Particle Abrasion at High Solids Concentration in Stirred Vessels—II," *Chem. Eng. Sci.*, **35**, 543 (1980).

Dalla Valle, J. M., and F. H. Goldman, "Volume-Shape Factor of Particulate Matter," *Ind. Eng. Chem., Anal. Ed.*, **11**, 545 (1939).

Diemer, R. B., Jr., "Moment Methods for Coagulation, Breakage and Coalescence Problems," Ph.D. Dissertation, Univ. of Delaware, Newark, DE (1999).

Diemer, R. B., and J. H. Olson, "A Moment Methodology for Coagulation and Breakage Problems: Part 3—Generalized Daughter Distribution Functions," *Chem. Eng. Sci.*, **57**, 4187 (2002).

Ennis, B. J., J. Green, and R. Davies, "Particle Technology: The Legacy of Neglect in the U.S.," *Chem. Eng. Prog.*, **90**(4), 32 (1994).

Gahn, C., J. Krey, and A. Mersmann, "The Effect of Impact Energy and the Shape of Crystals on Their Attrition Rate," *J. Cryst. Growth*, **166**, 1058 (1996).

Gahn, C., and A. Mersmann, "Brittle Fracture in Crystallization Processes. Part A and Part B," *Chem. Eng. Sci.*, **54**, 1273 (1999).

Gerstlauer, A., A. Mitrovic, S. Motz, and E.-D. Gilles, "A Population Model for Crystallization Processes Using Two Independent Particle Properties," *Chem. Eng. Sci.*, 56, 2553 (2001).

Hill, P. J., and K. M. Ng, "New Discretization Procedure for the Breakage Equation," *AIChE J.*, **41**, 1204 (1995).

Hill, P. J., and K. M. Ng, "Statistics of Multiple Particle Breakage," *AIChE J.*, **42**, 1600 (1996).

Hulburt, H. M., and S. Katz, "Some Problems in Particle Technology. A Statistical Mechanical Formulation," *Chem. Eng. Sci.*, **19**, 555 (1964).

Kendall, K., "The Impossibility of Comminuting Small Particles by Compression," *Nature*, **272**, 710 (1978).

Kousaka, Y., K. Okuyama, and A. C. Payatakes, "Physical Meaning and Evaluation of Dynamic Shape Factor of Aggregate Particles," *J. Colloid Interface Sci.*, **84**, 91 (1981).

Lohmander, S., "Influence of a Shape Factor of Pigment Particles on the Rheological Properties of Coating Colors," *Nordic Pulp & Paper Res. J.*, **15**, 231 (2000a).

Lohmander, S., "Influence of Shape and Shape Factor of Pigment Particles on the Packing Ability in Coating Layers," *Nordic Pulp & Paper Res. J.*, **15**, 300 (2000b).

Mazzarotta, B., "Abrasion and Breakage Phenomena in Agitated Crystal Suspensions," *Chem. Eng. Sci.*, **47**, 3105 (1992).

Mazzarotta, B., S. Di Cave, and G. Bonifazi, "Influence of Time on Crystal Attrition in a Stirred Vessel," *AIChE J.*, **42**, 3554 (1996).

Mersmann, A., *Crystallization Technology Handbook*, 2nd Edition, Marcell Dekker, New York (2001).
Molina-Boisseau, S., N. Le Bolay, and M. N. Pons, "Fragmentation Mechanism of Poly(vinyl acetate) Particles during Size Reduction in a Vibrated Bead Mill," *Powder Technol*., **123**, 282 (2002).
Mullin, J. W., *Crystallization*, 4th Edition, Butterworth-Heinemann, Boston (2001).
Nienow, A. W., and R. Conti, "Particle Abrasion at High Solids Concentration in Stirred Vessels," *Chem. Eng. Sci*., **33**, 1077 (1978).
Puel, F., P. Marchal, and J. Klein, "Habit Transient Analysis in Industrial Crystallization Using Two Dimensional Crystal Sizing Technique," *Trans. Inst. Chem. Eng*., **75**(Part A), 193 (1997).
Ramkrishna, D., *Population Balances: Theory and Applications to Particulate Systems in Engineering*, Academic Press, New York (2000).
Ramkrishna, D., and A. W. Mahoney, "Population Balance Modeling. Promise for the Future," *Chem. Eng. Sci*., **57**, 595 (2002).
Sathyagal, A. N., D. Ramkrishna, and G. Narsimhan, "Solution of Inverse Problems in Population Balances: II. Particle Break-up," *Comp. Chem. Eng*., **19**, 437 (1995).
Scanlon, M. G., and J. Lamb, "Fracture Mechanisms and Particle Shape Formation during Size Reduction of a Model Food Material," *J. Mater. Sci*., **30**, 2577 (1995).
Shamlou, P. A., A. G. Jones, and K. Djamarani, "Hydrodynamics of Secondary Nucleation in Suspension Crystallization," *Chem. Eng. Sci*., **45**, 1405 (1990).
Shamlou, P. A., Z. Liu, and J. G. Yates, "Hydrodynamic Influences on Particle Breakage in Fluidized Beds," *Chem. Eng. Sci*., **45**, 809 (1990).
Synowiec, P., A. G. Jones, and P. A. Shamlou, "Crystal Break-up in Dilute Turbulently Agitated Suspensions," *Chem. Eng. Sci*., **48**, 3485 (1993).
Wintermantel, K., "Process and Product Engineering: Achievements, Present and Future Challenges," *Trans. Inst. Chem. Eng*., **77**(Part A), 175 (1999).

Manuscript received Nov. 1, 2002, and revision received Aug. 8, 2003.